SEMARAK ILMU PUBLISHING

Semarak Journal of Thermal-Fluid Engineering

Journal homepage:
https://semarakilmu.my/index.php/sjotfe/index
ISSN: 3030-6639

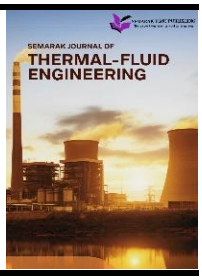

Analysis of Flow Through a Sudden Contraction in a Pipe

Henry Johnson[1,*]

[1] Faculty of Mechanical Engineering and Manufacturing, University Tun Hussein Onn Malaysia, 86400 Parit Raja, Johor, Malaysia

ARTICLE INFO

Article history:
Received 15 October 2025
Received in revised form 12 December 2025
Accepted 16 December 2025
Available online 21 December 2025

Keywords:
Sudden contraction; CFD; pressure drop; pipe flow; streamline analysis; ANSYS Fluent

ABSTRACT

Internal flow through sudden-contraction pipes is analysed using Computational Fluid Dynamics (CFD) in this work, with a sole focus on five flow characteristics: velocity contours, pressure contours, streamlines, velocity distributions, and pressure distributions. Three pipe layouts with identical total lengths and constant outlet diameters of 30 mm and intake diameters of 50, 60, and 70 mm were analysed. Without adding further complications unrelated to these fundamental fluid-dynamic phenomena, the goal of this work is to give a focused assessment of how input diameter affects flow acceleration, pressure loss, and downstream recovery. The finite volume approach was used to perform all simulations under steady, incompressible flow conditions. Although temperature gradients were not enforced, the governing equations included the continuity equation, momentum equation, and, for completeness, the energy equation. A grid independence test made sure that mesh refinement had no appreciable impact on numerical findings, and a uniform meshing method and solver configuration were used for all geometries. For all configurations, a zero-gauge outlet pressure, uniform inlet velocity, and no-slip wall conditions were employed to ensure that performance variations came only from geometric variation and not from boundary-condition effects. The findings demonstrate that narrower, high-momentum jet areas are produced at the contraction by sharper velocity gradients caused by smaller inlet diameters. Accordingly, the 70 mm inlet achieves the smoothest transition and the lowest hydraulic loss, while the 50 mm inlet case shows the biggest pressure drop because of the stronger flow acceleration. In contrast to the more uniform and connected flow produced by the 70 mm inlet, streamlines exhibit sharper curvature and tighter convergence in the smaller inlet instance, highlighting these features. These variations are quantified by the velocity and pressure distributions along the centrelines, demonstrating that jet strength, recovery duration, and pressure stabilization are all directly impacted by contraction intensity. This concentrated research shows that input diameter is a key factor in determining the flow behaviour caused by contraction and maximizing hydraulic efficiency.

1. Introduction

In industrial pipes, heat exchangers, hydraulic equipment, and process engineering systems, flow via abrupt contractions is a classic internal flow problem [1]. Jet formation, flow separation, and

* *Corresponding author.*
E-mail address: dd220053@student.uthm.edu.my

https://doi.org/10.37934/sjotfe.7.1.19a

severe shear layers are directly linked to the rapid acceleration and pressure loss that occur when a fluid passes through an abrupt fall in cross-sectional area [2]. These phenomena have a direct impact on mechanical loading, noise production, and energy efficiency in piping components [3]. These intricate flow patterns may now be thoroughly examined without depending just on experimental testing because to recent developments in computational fluid dynamics (CFD) [4]. CFD is especially useful for analysis contraction flows when steep gradients and localized effects predominate because it allows for the high-resolution observation of velocity and pressure fields [5]. Previous computational research has shown that downstream flow recovery and the shape of the vena contracta are significantly impacted by the contraction ratio [6]. Furthermore, it has been demonstrated that inlet geometry affects the degree of pressure loss and turbulence intensity throughout abrupt area changes [7].

Subsequently, few prior investigations isolate the effect of inlet diameter alone under controlled settings, whereas many concentrate on changing outlet diameter or contraction angle [8]. This necessitates focused research that compares the impact of input diameter while maintaining the same geometric and flow characteristics [9]. The optimization of compact piping systems and the reduction of hydraulic losses in industrial applications depend on an understanding of these interactions [10]. By examining flow through sudden-contraction pipes with inlet diameters of 50 mm, 60 mm, and 70 mm while keeping the outlet diameter and overall pipe length constant, the current study fills this gap. Only five essential flow characteristics such as velocity contours, pressure contours, streamline patterns, velocity distributions, and pressure distributions are examined [11,12].

2. Methodology

2.1 Geometry Modelling

Three straight circular pipes connecting to a sudden contraction portion were represented by the computational geometries that were created. Every model had a straight exit pipe, an abrupt contraction, and a straight inlet area [13]. To isolate the impact of intake geometry on flow behaviour, only the inlet diameter was altered (50 mm, 60 mm, and 70 mm) while the outlet diameter remained constant at 30 mm in all cases [14]. In order to guarantee flow development both prior to and following the contraction, enough upstream and downstream pipe lengths were incorporated [15]. Sharp-edged transitions, which are known to produce more jet effects and pressure losses than gradual contractions, were used to represent the contraction [16]. Table 1 below showed the three pipes sharing the same length and outlet diameter but with different inlet diameter.

Table 1
Dimension of three pipes with different inlet diameter

Pipe	Length (mm)	Inlet diameter (mm)	Outlet diameter (mm)
1	300	50	30
2	300	60	30
3	300	70	30

2.2 Mesh Development

The fluid domain was discretized using a hybrid structured–unstructured mesh to ensure both accuracy and computational efficiency. Fine grid spacing was imposed near the contraction plane since the region experiences the steepest velocity gradients. In the upstream and downstream straight sections, the mesh was gradually coarsened while maintaining adequate resolution near the

walls to capture boundary layer behaviour. The near-wall treatment ensured y^+ values in the recommended range for the turbulence model, aligning with guidelines from previous CFD literature [17].

A mesh independence assessment was conducted for all three configurations (Figure 1). Each pipe geometry was meshed at three different element sizes. For each level, key hydraulic metrics such as centreline velocity profiles and contraction-plane pressure drop were compared. Table 2 below showed the mesh configuration of each pipe with element size and nodes. When successive refinement produced changes below 2%, the mesh was accepted as sufficiently independent. This process avoids numerical diffusion while ensuring results were not excessively dependent on grid size [18-20].

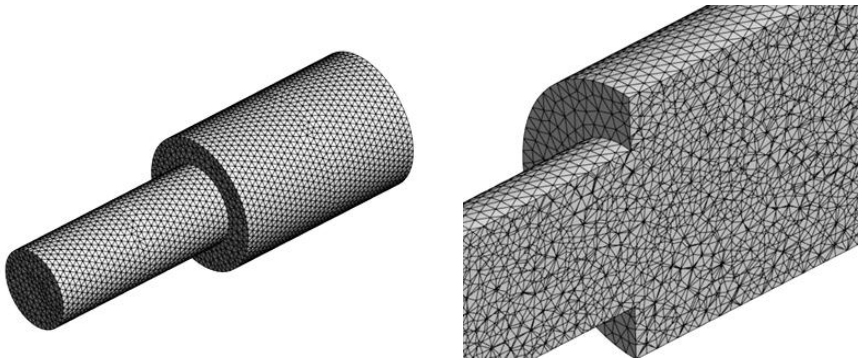

(a) (b)

Fig. 1. Mesh of pipe (a) Fluid domain (b) Detailed ross-section

Table 2
Mesh configuration for each pipe geometry

Pipe	Inlet diameter (mm)	Element size	Nodes
1	50	5.0	20,540
		4.0	39,468
		3.0	90,793
2	60	5.0	26,973
		4.0	51,429
		3.0	119,366
3	70	5.0	34,253
		4.0	65,771
		3.0	152,692

2.3 Governing Equations and Turbulence Modelling

All simulations solved the incompressible Navier–Stokes equations in their conservative form. The continuity Eq. (1) enforces mass conservation:

$$\nabla \cdot \mathrm{u} = 0 \tag{1}$$

and the momentum Eq. (2) accounts for convective transport, pressure gradients, and viscous stresses:

$$\rho(\mathrm{u} \cdot \nabla)\mathrm{u} = -\nabla p + \mu \nabla^2 \mathrm{u} \tag{2}$$

Due to the presence of strong shear layers and turbulent mixing in the contraction zone, the standard k–ε turbulence model was selected. Although more advanced models exist, k–ε is widely validated for internal flows and offers stable performance with moderate computational cost [20]. Its two-equation formulation solves for turbulent kinetic energy (k) and turbulent dissipation rate (ε), enabling representation of isotropic turbulence effects in the flow.
The Reynolds number of the flow was evaluated using:

$$Re = \frac{\rho UD}{\mu} \tag{3}$$

where D corresponds to the inlet diameter of each pipe.

2.4 Boundary and Solver Conditions

A uniform velocity inlet was applied at the upstream boundary of each pipe. Although real pipe flow typically exhibits a parabolic profile, the straight inlet length ensured sufficient distance for boundary layer development prior to the contraction. A no-slip condition was imposed at all walls. At the outlet, a zero-pressure boundary condition allowed the flow to exit freely while maintaining numerical stability. The SIMPLE algorithm was employed for pressure–velocity coupling. Momentum equations were discretized using a second-order upwind scheme to ensure high spatial accuracy without inducing instability. Convergence was assessed using both residual levels (target: 1×10^{-6}) and the stabilization of monitored flow variables.

3. Results

3.1 Grid Independence Test (GIT)

The three pipe layouts exhibit identical trends in the combined velocity and pressure distribution graphs. Because of the considerable acceleration brought on by the higher contraction ratio, the 50 mm inlet generates the highest peak velocity and the sharpest pressure drop. While the 70 mm intake displays the minimum pressure loss and the lowest velocity peaks, suggesting a smoother flow transition and quicker recovery, the 60 mm inlet displays intermediate behaviour. These graph patterns demonstrate that while bigger intake diameters encourage more steady velocity development and better pressure performance, smaller inlet diameters increase flow acceleration and hydraulic losses.

The comparative results show that inlet diameter significantly influences the flow topology within the contraction. Smaller diameters produce sharper velocity gradients and steeper pressure drops, while larger diameters generate smoother flow transitions. These findings corroborate prior experimental observations on internal contraction flows and reinforce the importance of optimizing inlet size to minimize energy losses in engineering applications.

3.1.1 Velocity distribution

Velocity distributions along the pipe centreline were plotted together to provide direct comparison in Figure 2. The 50 mm inlet shows the sharpest velocity spike at the contraction, followed by a long decay region where the flow transitions from jet-like to fully developed. The 60 mm inlet demonstrates a smoother peak and shorter decay. The 70 mm inlet produces the broadest acceleration region but the smallest peak magnitude, indicating a less aggressive jet formation. Such differences are consistent with contraction-driven jet behaviour described in previous CFD analyses.

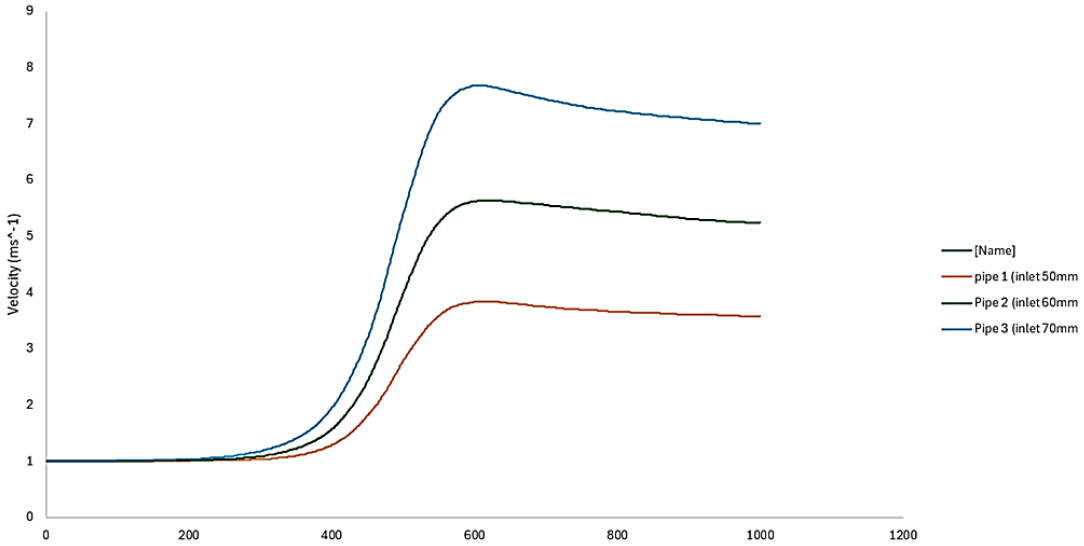

Fig. 2. Velocity distribution of three pipes

3.1.2 Pressure distribution

The pressure distribution plot highlights the relationship between inlet diameter and head loss shown in Figure 3. The smallest inlet yields the largest drop at the contraction, reflecting greater energy losses. The 60 mm inlet creates moderate losses, while the 70 mm inlet minimizes pressure discontinuity. Downstream, the pressure recovery rate depends on the turbulence structure and reattachment length. Larger inlets recover pressure more quickly, demonstrating superior hydraulic efficiency.

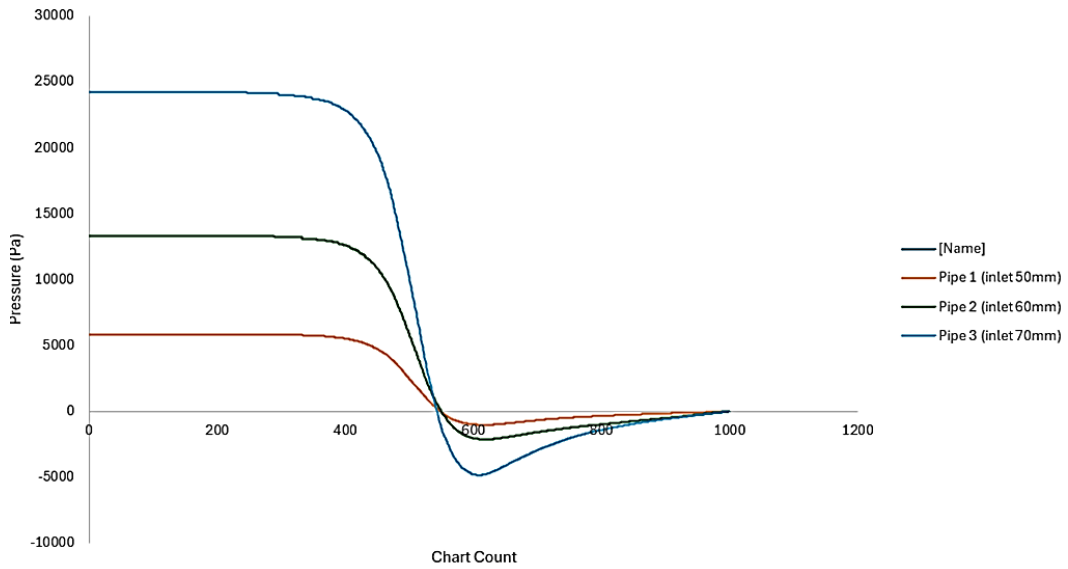

Fig. 3. Pressure distribution of three pipes

3.2 Velocity Contours

Velocity contours clearly illustrate how fluid acceleration differs among the three inlet diameters. For the 50 mm inlet configuration, the contraction ratio is highest, producing a pronounced jet immediately downstream of the contraction. This jet remains narrow and energetic for a longer

distance before being dissipated by turbulent mixing. Similar behaviour has been observed in prior studies of high contraction-ratio flows.

For the 60 mm inlet, the velocity peak at the contraction is still significant but less intense, producing a slightly shorter jet core. The 70 mm inlet shows the smoothest acceleration process, with the widest jet core but the least severe velocity gradients. This behaviour suggests that larger inlet diameters promote more uniform upstream velocity distributions, reducing the severity of contraction-plane flow acceleration. The velocity contour of the three pipe is shown in the Figure 4 below.

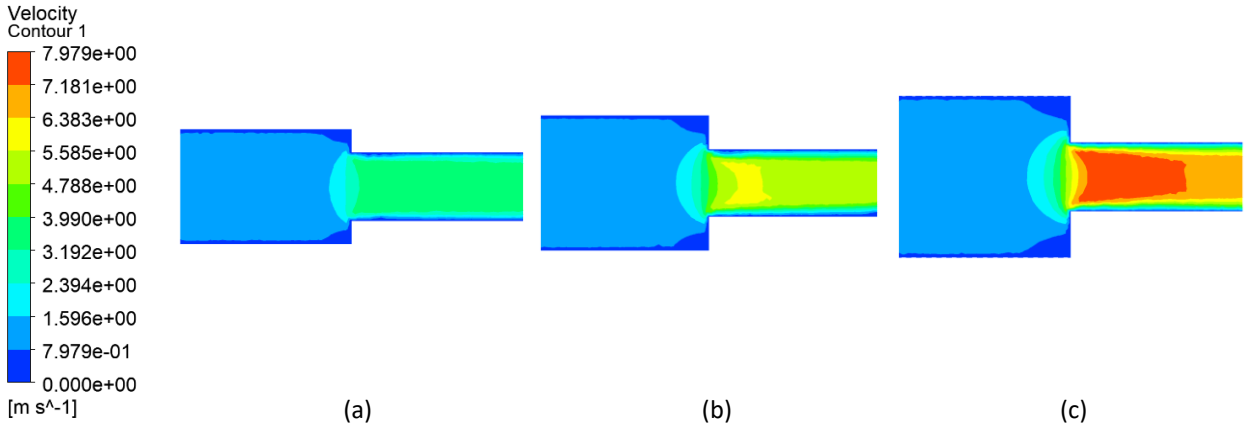

Fig. 4. Velocity contour of inlet (a) 50 mm (b) 60 mm (c) 70 mm

3.3 Pressure Contours

Pressure contours reveal that the most severe pressure drop occurs in the 50 mm inlet configuration. This aligns with theoretical predictions that the loss coefficient increases with contraction ratio. The abrupt velocity rise in the smallest inlet case creates a stronger adverse pressure gradient, intensifying local energy losses. The 60 mm inlet shows a moderate pressure drop, whereas the 70 mm inlet exhibits the mildest reduction in static pressure. Beyond the contraction, pressure recovery occurs as the flow reattaches to the pipe wall. Recovery is fastest in the 70 mm configuration due to its smoother acceleration and thicker jet structure. Figure 5 below show the pressure contour of three pipe.

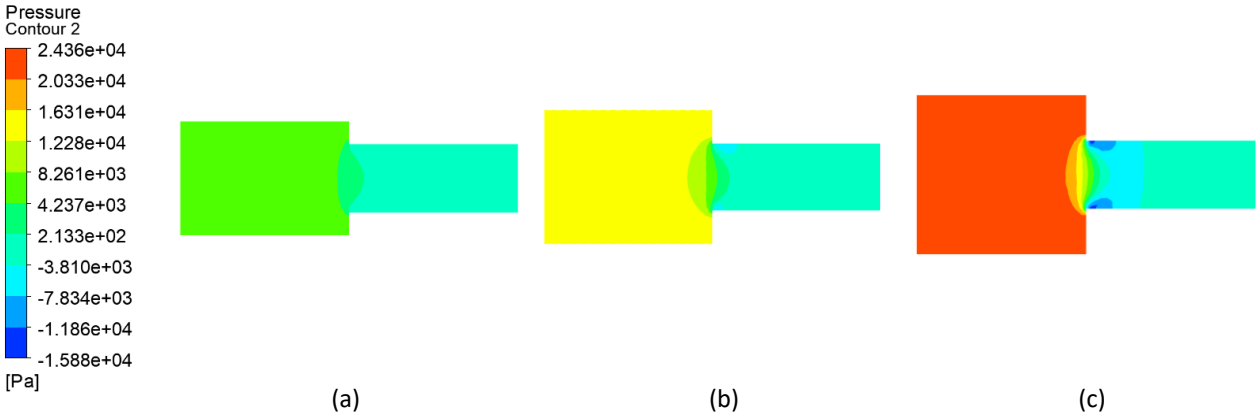

Fig. 5. Pressure contour of inlet (a) 50 mm (b) 60 mm (c) 70 mm

3.4 Streamline Analysis

The streamline patterns for the three pipe configurations illustrate how inlet diameter influences flow organization through and beyond the contraction as shown in Figure 6. In the 50 mm inlet case, the streamlines converge sharply toward the contraction and form a narrow jet that induces noticeable curvature and a small separation region near the wall downstream. The 60 mm inlet exhibits smoother convergence, producing milder curvature and only limited near-wall disturbance. In contrast, the 70 mm inlet generates the most uniform streamline behaviour, with minimal deviation and no significant separation, reflecting a more stable and energetically efficient flow transition. Overall, the streamline visualizations confirm that larger inlet diameters promote more attached and orderly flow, while smaller inlets amplify curvature, acceleration, and localized separation effects.

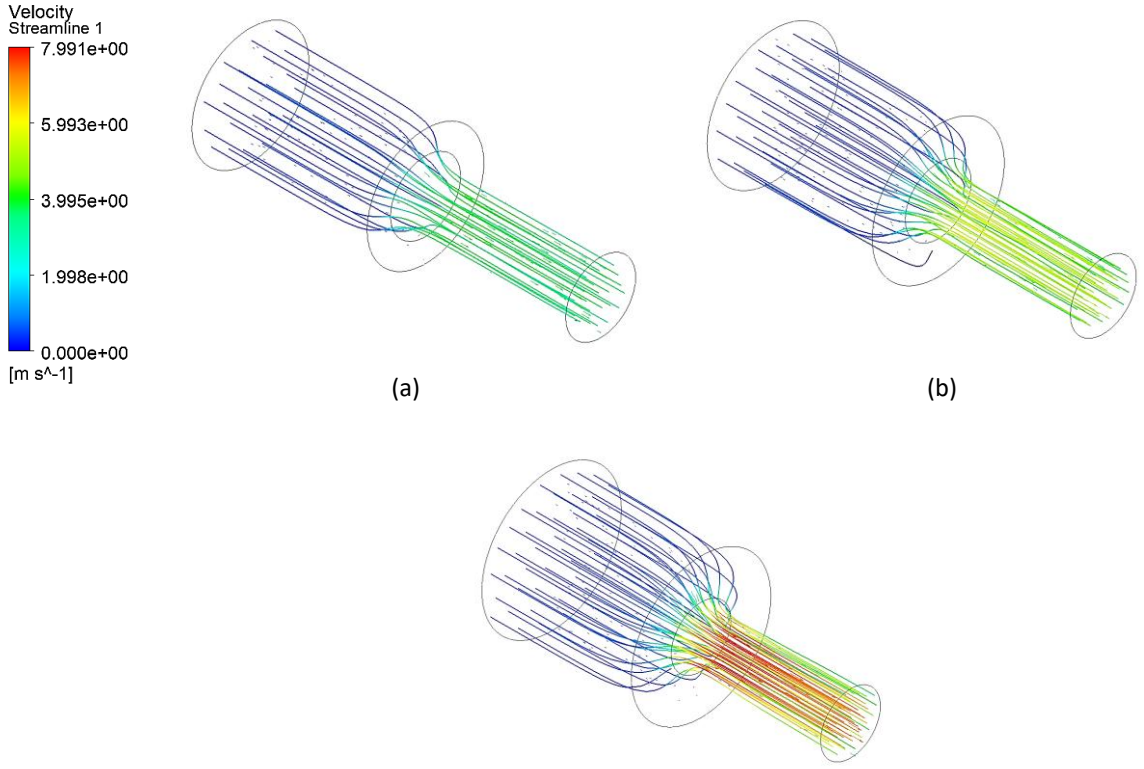

Fig. 6. Streamline of inlet (a) 50 mm (b) 60 mm (c) 70mm

4. Conclusions

This study assessed the effects of inlet diameter on the flow behaviour of sudden contraction pipes using CFD simulations. Across three configurations (50 mm, 60 mm, and 70 mm inlets), all converging to a 30 mm outlet, substantial variation in flow acceleration, jet formation characteristics, pressure losses, and downstream recovery was observed. The smallest inlet produced the most intense flow acceleration and greatest pressure drop, consistent with established contraction-flow theory. Meanwhile, the largest inlet enabled smoother flow development and lower hydraulic losses, supporting conclusions drawn by previous CFD researchers. These results illustrate the significance of inlet geometry in influencing flow efficiency and provide practical guidance for the design of piping systems requiring sudden cross-sectional transitions.

References

[1] Togun, Hussein, Tuqa Abdulrazzaq, S. N. Kazi, A. Badarudin, and Mohd Khairol Anuar Ariffin. "Numerical study of turbulent heat transfer in annular pipe with sudden contraction." *Applied Mechanics and Materials* 465 (2014): 461-466. https://doi.org/10.4028/www.scientific.net/AMM.465-466.461

[2] Chakkour, T. (2022). Numerical simulation of pipes with an abrupt contraction using openfoam. *Fluid Mechanics at Interfaces 2: Case Studies and Instabilities*, 45-75. https://doi.org/10.1002/9781119903000.ch3

[3] Jana, Arun, and Girish D. Vegad. "Computational fluid dynamics-based study on the heavy crude oil-water emulsion flow through sudden expansion, contraction and 90° bend." *Journal of Mechanical Engineering and Sciences* (2024): 9976-9987. https://doi.org/10.15282/jmes.18.2.2024.1.0788

[4] Banerjee, Shirsendu, Anirban Banik, Vinay Kumar Rajak, Tarun Kanti Bandyopadhyay, Jayato Nayak, Michał Jasinski, Ramesh Kumar, Byong-Hun Jeon, Masoom Raza Siddiqui, Moonis Ali Khan, Sankha Chakrabortty, and Suraj K. Tripathy "Two-phase crude oil–water flow through different pipes: an experimental investigation coupled with computational fluid dynamics approach." *ACS Omega* 9, no. 10 (2024): 11181-11193. https://doi.org/10.1021/acsomega.3c05290

[5] Gulsacan, Burak, Nehir Tokgoz, Enver S. Karakas, Matteo Aureli, and Cahit A. Evrensel. "Effect of orifice thickness-to-diameter ratio on turbulent orifice flow: An experimental and numerical investigation." *International Communications in Heat and Mass Transfer* 151 (2024): 107213. https://doi.org/10.1016/j.icheatmasstransfer.2023.107213

[6] Shi, Jing, Mustapha Gourma, and Hoi Yeung. "A CFD study on horizontal oil-water flow with high viscosity ratio." *Chemical Engineering Science* 229 (2021): 116097. https://doi.org/10.1016/j.ces.2020.116097

[7] Bandarra Filho, Enio Pedone, Erick Oliveira do Nascimento, Muhammad Farooq, and Luben Cabezas-Gómez. "Numerical investigation on heat transfer and pressure drop in silver/water nanofluids flowing through tubes with variable expansion–contraction ratios." *Energies* 18, no. 1 (2025): 161. https://doi.org/10.3390/en18010161

[8] Daneshfaraz, Rasoul, Ehsan Aminvash, Reza Esmaeli, Sina Sadeghfam, and John Abraham. "Experimental and numerical investigation for energy dissipation of supercritical flow in sudden contractions." *Journal of groundwater science and engineering* 8, no. 4 (2020): 396-406. https://doi.org/10.19637/j.cnki.2305-7068.2020.04.009

[9] Abdulrazzaq, Tuqa, Hussein Togun, Marjan Goodarzi, S. N. Kazi, M. K. A. Ariffin, N. M. Adam, and Kamel Hooman. "Turbulent heat transfer and nanofluid flow in an annular cylinder with sudden reduction." *Journal of Thermal Analysis & Calorimetry* 141, no. 1 (2020). https://doi.org/10.1007/s10973-020-09538-6

[10] Patra, Saroj K., Manmatha K. Roul, Prasanta K. Satapathy, and Ashok K. Barik. "Fluid dynamics and pressure drop prediction of two-phase flow through sudden contractions." *Journal of Fluids Engineering* 143, no. 9 (2021): 091401. https://doi.org/10.1115/1.4050962

[11] Sauvage, Bastien, Frédéric Alauzet, and Alain Dervieux. "A space and time fixed point mesh adaptation method." *Journal of Computational Physics* 519 (2024): 113389. https://doi.org/10.1016/j.jcp.2024.113389

[12] Gopal, Arul Nalmanan Raja. "Comparative study of internal flow dynamics using CFD for of sudden expansion pipe." *Journal of Advances in Fluid, Heat, and Materials Engineering* 5, no. 1 (2025): 37-44. https://doi.org/10.37934/afhme.5.1.3744a

[13] Xu, Dong, Jianing Liu, Yunfeng Wu, and Chunning Ji. "A high-efficiency discretized immersed boundary method for moving boundaries in incompressible flows." *Scientific Reports* 13, no. 1 (2023): 1699. https://doi.org/10.1038/s41598-023-28878-5

[14] Powar, Omkar, Pedapudi Anantha Hari Arun, Anwak Manoj Kumar, Mithun Kanchan, B. M. Karthik, Poornesh Mangalore, and Mohith Santhya. "Recent developments in the immersed boundary method for complex fluid–structure interactions: A Review." *Fluids* 10, no. 5 (2025): 134. https://doi.org/10.3390/fluids10050134

[15] Kumar, Ashutosh, and Mukesh Sharma. "Effect of liquid-liquid flows on flow pattern, pressure drop, wall shear drop, and strain rate drop through sudden contraction and expansion pipe coupled with return bend: A CFD analysis." *Experimental and Computational Multiphase Flow* 7, no. 1 (2025): 109-120. https://doi.org/10.1007/s42757-023-0169-7

[16] Sun, H., X. Zhu, X. Wang, J. Zhao, S. Hu, and J. Yu. "A Study on a semi-empirical model for the local loss coefficient of small angle contraction pipes." *Journal of Applied Fluid Mechanics* 18, no. 6 (2025): 1446-1458. https://doi.org/10.47176/jafm.18.6.3249

[17] Wen, J., Y. Ren, D. Wang, and C. Bai. "Experimental and numerical investigation on gas–liquid two-phase flow dynamics and pressure drop in horizontal contraction pipes." *Journal of Applied Fluid Mechanics* 18, no. 12 (2025): 3082-3100. https://doi.org/ 10.47176/jafm.18.12.3597

[18] Sadek, Samir H., Fernando T. Pinho, and Manuel A. Alves. "Electro-elastic flow instabilities of viscoelastic fluids in contraction/expansion micro-geometries." *Journal of Non-Newtonian Fluid Mechanics* 283 (2020): 104293. https://doi.org/10.1016/j.jnnfm.2020.104293

[19] Mugundhan, Vivek, and Sigurdur T. Thoroddsen. "Circulation in turbulent flow through a contraction." *Journal of Turbulence* 24, no. 11-12 (2023): 577-612. https://doi.org/10.1080/14685248.2023.2284187

[20] Nohmi, Motohiko, Shusaku Kagawa, Tomoki Tsuneda, Wakana Tsuru, and Kazuhiko Yokota. "Numerical analysis of contraction geometry effects on cavitation choking in a piping system." In *Fluids Engineering Division Summer Meeting*, vol. 59056, p. V03BT03A033. American Society of Mechanical Engineers, 2019. https://doi.org/10.1115/AJKFluids2019-5359